ISSN 1063-7842, Technical Physics, 2016, Vol. 61, No. 4, pp. 563–568. © Pleiades Publishing, Ltd., 2016.
Original Russian Text © A.P. Vladimirov, I.S. Kamantsev, V.E. Veselova, E.S. Gorkunov, S.V. Gladkovskii, 2016, published in Zhurnal Tekhnicheskoi Fiziki, 2016, Vol. 86, No. 4, pp. 85–90.

SOLID STATE

Use of Dynamic Speckle Interferometry for Contactless Diagnostics of Fatigue Crack Initiation and Determining Its Growth Rate

A. P. Vladimirov, I. S. Kamantsev, V. E. Veselova, E. S. Gorkunov, and S. V. Gladkovskii

Institute of Engineering Science, Ural Branch, Russian Academy of Sciences, Yekaterinburg, 620049 Russia

e-mail: ks@imach.uran.ru

Received July 28, 2015

Abstract—Steel 09G2S specimens are subjected to cyclic tests, and real-time monitoring of the initiation of a fatigue crack and its growth kinetics is performed by dynamic speckle interferometry. The time averaging of speckles are used to reveal a relation between the parameters that characterize random and deterministic changes in the relief height and speckle images of the surface near the notch during crack initiation.

DOI: 10.1134/S106378421604023X

INTRODUCTION

Various coherent optical methods, such as holographic interferometry [1], correlation interferometry [2], dynamic speckle interferometry [3], and the methods based on shift [4] and change of speckle fields [5], are now applied in experimental fracture mechanics to determine the macroscopic displacement, the elastic deformation, the rotation, and the velocity of an object [6].

The results obtained in [7–9] show that the use of these methods for an investigation of fatigue phenomena causes some problems related to the necessity of recording a large number of holograms and speckle patterns and to the nonmonotonic character of evolution of detected parameter with the number of loading cycles. Therefore, these methods have not found wide use in studying the processes that occur in materials subjected to cyclic loading.

This restriction can be lifted by time averaging of speckles to study the high-cycle fatigue of metals. It was shown [10] that time averaging of speckles substantially simplifies experiments, since it can be used to investigate fatigue processes without termination of cyclic loading.

The authors of [10] also revealed a relation between the change of the relief in the macroscopic fracture nucleation zone and the change in the time-averaged speckle image of this zone. In terms of the key concepts of fracture mechanics, a change in the surface relief at a crack tip during cyclic loading is related to the formation of a localized plastic deformation zone (LPDZ) [11]. The size and shape of the plastic zone are determined by the following factors: the state of stress, the plastic deformation resistance of a material, the strain-hardening exponent, and stress intensity factor K (or its peak-to-peak amplitude ΔK in the case of cyclic loading) operating at a crack tip. The following two types of LPDZ at the tip of a growing crack are distinguished during cyclic loading: an extended monotonic static plastic zone and a cyclic plastic zone inside it [12].

As follows from [10], the LPDZ sizes determined with a profilometer and from a change in a speckle field coincide to an accuracy of ±44 μm. Since the change in the relief behind the tip of a crack stabilizes gradually after its initiation and then terminates, this effect can be used to determine the fatigue crack velocity. Nevertheless, the formation of LPDZ during the nucleation of a fatigue crack has not been studied in detail. The purpose of this work is to investigate the formation of LPDZ during fatigue crack (FC) nucleation by dynamic speckle interferometry and to develop a technique of determining the crack velocity from the LPDZ increment at the crack tip.

EXPERIMENTAL

We studied prismatic low-carbon 09G2S steel specimens 55 mm long, 5 mm wide, and 10 mm high. A sharp V-shaped notch 2 mm wide with a radius of curvature of 0.25 mm at its tip was made in a specimen to localize the site of possible FC initiation. After preliminary mechanical treatment (milling and grinding followed by vacuum annealing), the surface to be studied was subjected to polishing to create a mirror surface with a roughness parameter $R_a = 1–50$ nm.

Cyclic loading was performed on a high-frequency MIKROTRON (RUMUL) resonance testing machine according to the three-point bending scheme at a maximum cycle force of 1.2 kN, a loading frequency of ≈100 Hz, and a stress ratio $R = 0.1$.

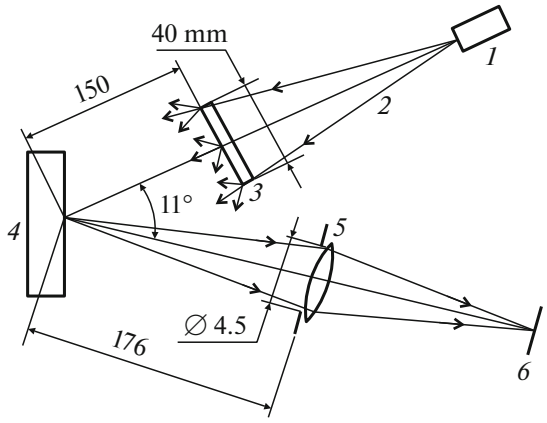

Fig. 1. Schematic diagram of the optical setup: (*1*) laser unit, (*2*) illuminating radiation, (*3*) clouded glass, (*4*) specimen, (*5*) lens with aperture, and (*6*) TV camera photodetector matrix.

To detect speckle fields, we used an optical system, the scheme and the geometric sizes of which are shown in Fig. 1. The optical system was mounted on the platform of the testing machine. Object *4* was illuminated by beam *2* from KLM-H650-40-5 laser unit *1* with a wavelength of 0.65 μm and a power of 40 mW. Clouded glass *3* was introduced into the illuminating beam to form speckle fields in the case of specimens with a polished surface, since speckles do not form when a mirror surface is illuminated. A speckle pattern was recorded in the specimen image plane. The optical system magnification was 0.7. The aperture size of lens *5* was chosen so that the minimum speckle size was slightly larger than the photoelectric cell size in TV camera photodetector matrix *6*. In experiments, we used a monochrome VIDEOSKAN-415M-USB TV camera with a matrix containing 782 × 582 photocells 8.3 × 8.3 μm in size.

In the method of averaging speckles, exposure time τ_0 of the TV camera was chosen to be equal to or a multiple of cyclic loading period T. At $\tau_0 = T$, an element in the TV camera photodetector matrix responds to the radiation intensity averaged over time interval T. If irreversible processes do not occur in the object, digitized signals are unchanged in the next T time intervals. Such signals will change if irreversible processes, which change the surface microrelief of the object and, hence, its speckle field, appear at any phase of object vibration.

In experiments, the chosen exposure time of the TV camera corresponded to 50 loading cycles. Speckle image frames were recorded in the BMP graphical format 1000–2500 loading cycles after the resonance frequency of the testing machine was stabilized. As the parameter that characterizes a change in speckles, we chose coefficient of correlation η of two 8-bit digital images of the same dimension. The digital images were represented by two-dimensional matrices corresponding to a certain frame region at initial time t_1 and current time t_2 at N_1 and N_2 loading cycles, respectively. The values of η were found by the formula

$$\eta = \frac{\frac{1}{nm}\sum_{i=0}^{n-1}\sum_{j=0}^{m-1}(A_{ij}-\bar{A})(B_{ij}-\bar{B})}{\left(\frac{1}{nm}\sum_{i=0}^{n-1}\sum_{j=0}^{m-1}(A_{ij}-\bar{A})^2\right)^{1/2}\left(\frac{1}{nm}\sum_{i=0}^{n-1}\sum_{j=0}^{m-1}(B_{ij}-\bar{B})^2\right)^{1/2}}, \quad (1)$$

where i and j are the row element (pixel) number and the matrix row number, respectively; n and m are the number of row pixels and the number of matrix rows, respectively; A_{ij} is the value of the pixel with numbers i and j at t_1; B_{ij} is the value of this pixel at time t_2; $\bar{A}$ is the arithmetical mean of the values of the matrix elements at t_1; and $\bar{B}$ is the arithmetical mean of the values of the matrix elements at time t_2.

As follows from Eq. (1), η is unity in the absence of any differences between two speckle images. The experience showed [10] that η vanishes upon random changes of 100 nm in the relief heights with respect to the initial value. An intermediate value of the coefficient of correlation from unity to zero corresponds to smaller changes in the relief height. The value of η is –1 in time $T/2$ if the radiation intensity in each pixel changes as a cosine at the same period T and different initial phases.

To record surface profiles and to determine the root-mean-square deviation of the relief heights in a chosen region, a specimen was periodically removed from the testing machine for its surface to be analyzed on a WYKO NT-1100 optical profilometer at a height measurement error of 3 nm. Once a crack moved, the position of its tip was determined when the specimen was illuminated by radiation from a white light source, and laser radiation was shut in this case.

RESULTS AND DISCUSSION

Based on experimental data, we plotted coefficient of correlation η distributions for speckle images. Figure 2 shows typical η distributions in the range 0.6–1.0 at various stages of formation of LPDZ near

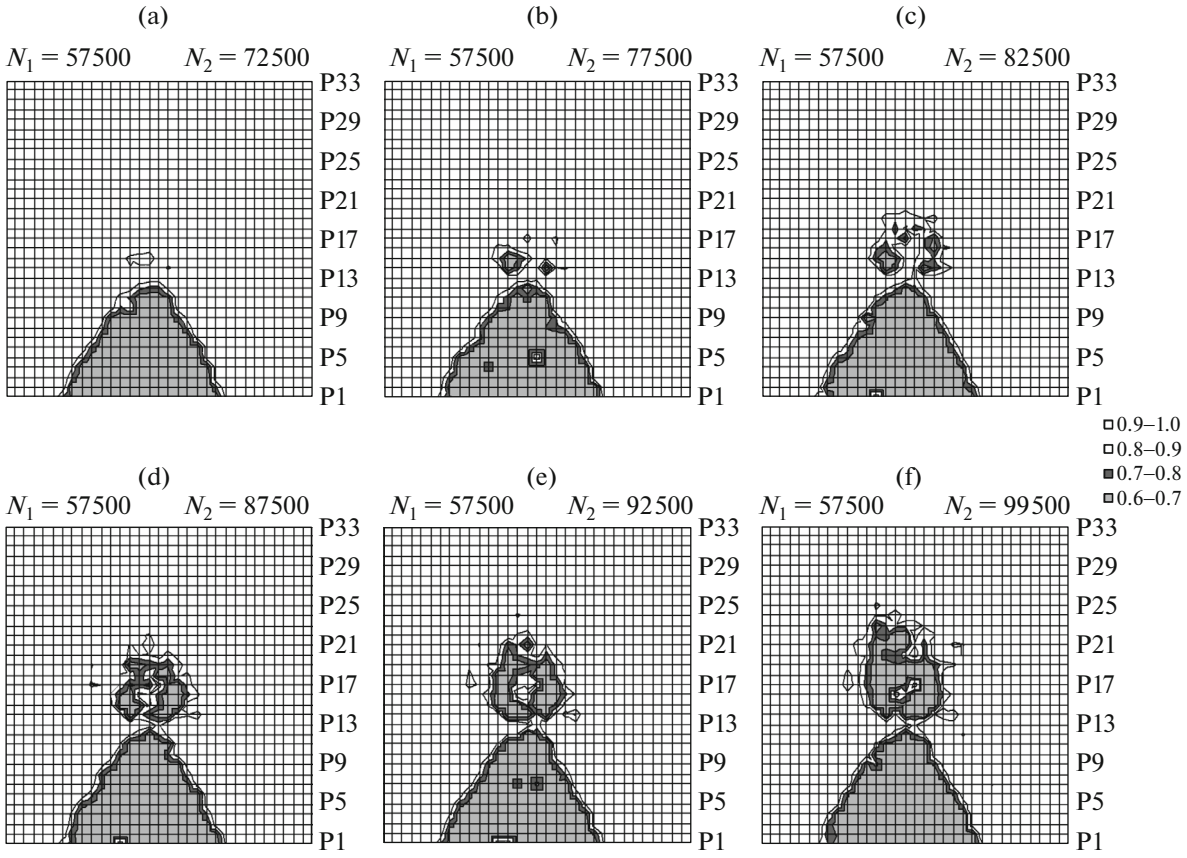

Fig. 2. η distributions at various numbers of loading cycles.

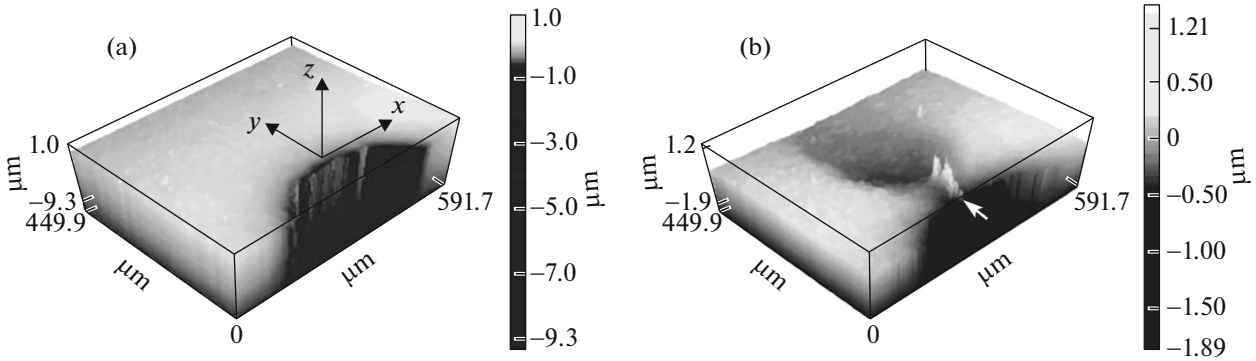

Fig. 3. Three-dimensional surface profiles near a notch at N = (a) 57 500 and (b) 99 500.

the notch tip. As is seen from these data, the first changes of η near the image of the notch tip appear at N = 77 500 cycles (Fig. 2b). On the following loading, the region in which the change of η was in the range 0.6–1 grew gradually. A comparison of η with the three-dimensional (Fig. 3) and two-dimensional (Fig. 4) surface profiles showed that the maximum changes of η, which were designated as η_{max}, were at the steepest valley slopes of the valley formed near the notch tip. In Fig. 4, Δh is the difference between the relief heights found from the two surface profiles corresponding to $N_1 = 57\,500$ and $N_2 = 99\,500$ loading cycles. The values of η were found from digital images 4 × 4 pixels in size. Coordinate x corresponded to the center of the digital image.

The maximum valley depth was about 1 μm and the longitudinal and transverse sizes were several hundred microns. Figure 5 shows η_{max} versus the maximum slope of the surface γ_{max} plotted from five surface pro-

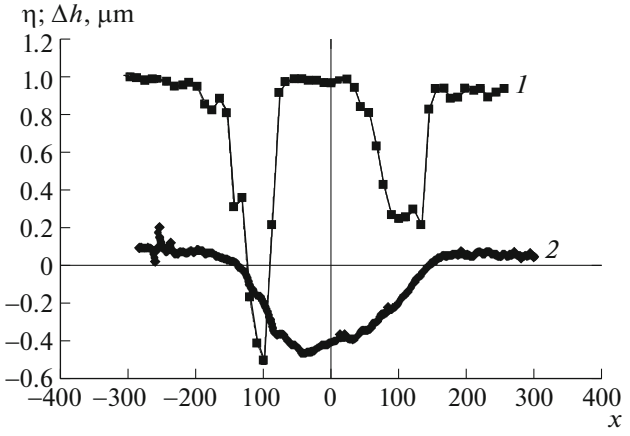

Fig. 4. Superimposed dependences of (*1*) coefficient of correlation η and (*2*) difference in the relief heights Δh on coordinate x.

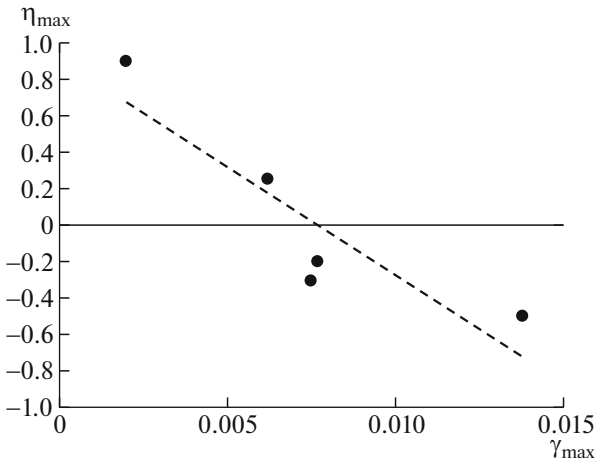

Fig. 5. Experimental values of η_{max} vs. γ_{max}.

files. The value of γ_{max} was graphically found from the $\Delta h(x)$ dependence. If γ_{max} is considered as the measure of plastic deformation, the dependence of η_{max} on γ_{max} can be used to estimate it roughly.

As follows from Fig. 3b, a 50-μm zone, which is designated by an arrow and has a relief that differs substantially from the surrounding relief, exists at the notch tip. Relief heterogeneities in the form of characteristic projections with a cross section of 5–10 μm and a height up to several hundred nanometers are observed inside this zone. Optical microscopy data showed that a fatigue crack initiated in this zone.

A comparison of the dynamics of speckle fields and the surface relief in the range 57500–99500 loading cycles showed that the changes of η were caused by the following four factors:

(1) Small translational displacements of the object, which are likely to be related to the appearance of residual strains. Such displacements caused a decrease in η from 1.0 to 0.99.

(2) Small changes in the surface roughness inside the valley, which increase parameter R_a by several tens of nanometers when η decreases by approximately 0.05.

(3) Chaotic changes in the relief height by several hundred nanometers in the fatigue crack initiation zone, which result in a change in η in this zone up to 0.7–0.8.

(4) Deterministic changes in the surface relief during the formation of a 1-μm-deep valley, where the changes of η to negative values of –0.5 were detected in the steepest valley slopes.

The significant changes in η in the images of the regions where the surface relief changes not randomly are likely to be explained as follows. We now consider the motion of surface points in a small region, which is located in the steep valley slope and the size of which is equal to the linear resolution of the lens (11 μm). To a first approximation, the region motion can be considered as the sum of the following three types of motion: translational motion along axis z, uniform deformation, and rigid rotation about the axis perpendicular to axis z (Fig. 3a). For illumination and observation along the normal to the surface, the first two types of motion do not change the difference between the phases of the wave pairs reflected from different centers of scattering located in the region. The phase difference changes during rigid rotation of the region. We now consider the centers of scattering located randomly toward the axis of rotation at the same desistance from each other in the direction normal to the axis of rotation. The initial phases of the waves reflected from such centers should be the same. Then, during rigid rotation of the region, interference of many waves reflected from these centers appears as in a diffraction grating. The difference consists in the fact that a quasi-periodic change in radiation intensity in the case of a diffraction grating occurs in space and such a change in our experiments occurs in one pixel in time. Since a similar situation takes place in neighboring pixels, quasi-periodic changes in signals also appear in them. Elementary estimates demonstrate that η becomes –1 in one-half period if periodic changes in intensity I occur in all pixels at the same frequency and different initial phases. A comparison of signals in different pixels showed that dependences $I = I(N)$ are not strictly periodic, and the negative correlation of speckle fields reaches only –0.5.

The experimental results demonstrate that it is convenient to observe the changes that occur in the plastic deformation zone by comparing speckle image frames recorded in 2500–5000 cycles. An analysis of the distributions of the values of η thus found showed that all changes up to $N = 107\,500$ cycles were observed inside the valley. Beginning from $N = 107\,500$, the field of the value of η corresponding to an increment of plastic deformation moves. This fact is assumed to

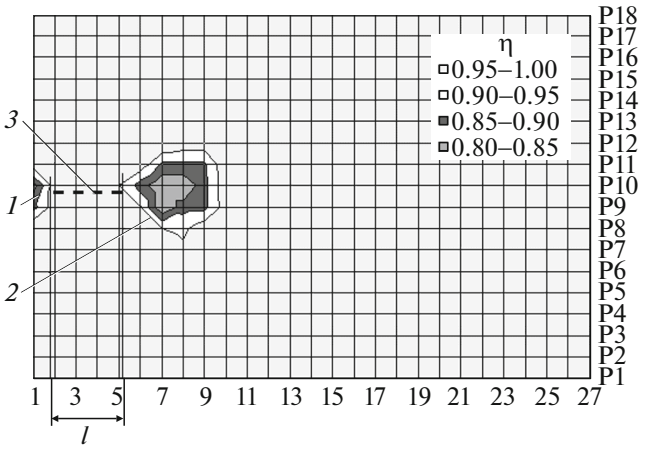

Fig. 6. η field in the specimen image plane: (*1*) notch tip, (*2*) growth of the plastic deformation zone, and (*3*) fatigue crack. The step of grid along axes *x* and *y* is 10 pixels.

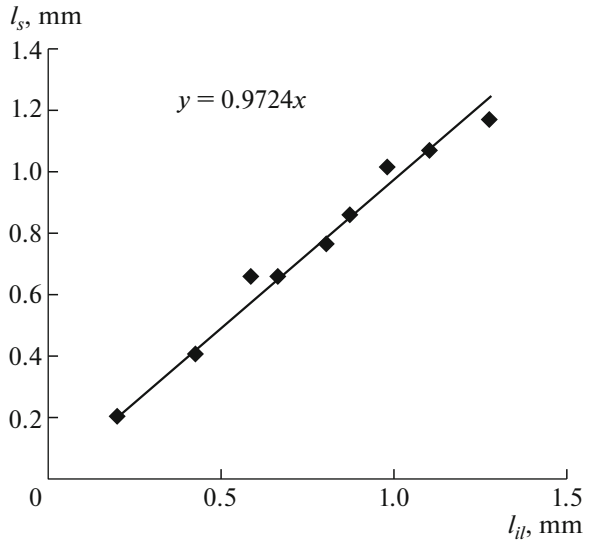

Fig. 7. Comparison of the fatigue crack length determined from a change in a speckle field (l_s) and during illumination by white light (l_{il}).

correspond to crack initiation. Figure 6 shows an η distribution, which was obtained during macrocrack propagation and demonstrates the growth of the plastic deformation zone The observations performed on a polished specimen showed that the boundary of changes in η that is nearest to the notch approximately coincides with the image of the crack tip. We assumed that this circumstance can be used to determine the dependence of crack length *l* on the number of loading cycles *N*.

To check the correctness of this assumption, we compared two dependences of *l* on *N* found by dynamic speckle interferometry and a traditional optical method. The first dependence was determined from a change in the field of η corresponding to the growth of plastic deformation zone, and the second dependence was determined during the observation of the specimen surface illuminated by white light. As is seen in Fig. 7, the fatigue crack lengths determined by different methods agree well with each other. Thus, our experimental results demonstrate a high efficiency of using dynamic speckle interferometry to study the growth a fatigue crack in metallic materials during cyclic loading. The advantage of determining the length and the velocity of a fatigue crack from the correlation of speckle images is the possibility of application of this experimental approach to specimens with a rough surface, where a crack can hardly be detected by optical methods.

CONCLUSIONS

When performing time averaging of speckles during cyclic loading of a steel 09G2S specimen with a sharp notch under high-cycle fatigue conditions, we were able to reveal a relation between the parameters that characterize random and deterministic changes in the relief height and speckle images of the surface near the notch during crack initiation. These parameters are roughness R_a, change in the surface relief height Δh, and coefficient η of correlation of speckle images.

The following conclusions can be drawn from our experimental results.

(1) Crack initiation at the notch tip is accompanied by gradual formation of a plastic zone in the form of a valley 50–700 μm in diameter of depth $\Delta h = 1$ μm.

(2) Coefficient η of correlation of speckle images is determined by the following factors arranged in order of increasing importance: small translational motion of the surface, small changes in the surface roughness within the plastic zone (change of R_a by several tens of nanometers), significant random changes in the surface relief in the crack initiation zone (change of R_a by several hundred nanometers in a region 50–100 μm in size), and changes in the surface relief within the plastic zone. The maximum changes of η correspond to the surface regions located in the steepest slopes of the valley.

(3) It was shown that the fatigue crack growth rate can be determined without termination of cyclic loading from the parameter η distributions corresponding to the growth of the plastic deformation zone in 2000 loading cycles.

ACKNOWLEDGMENTS

The studies were performed using the equipment of the Center of Joint Use Plastometry of the Institute of Engineering Science was supported in part by the Russian Foundation for Basic Research (project no. 14-

08-31673mol_a) and basic research projects 15-10-1-22 and 15-7-120 of the Ural Branch, Russian Academy of Sciences.

REFERENCES

1. E. B. Aleksandrov and A. M. Bonch-Bruevich, Sov. Phys. Tech. Phys. **12**, 258 (1967).
2. J. A. Leendertz, J. Phys. E: Sci. Instrum. **3**, 214 (1970).
3. A. P. Vladimirov and V. I. Mikushin, Proc. SPIE **3726**, 38 (1999).
4. I. Yamaguchi, Opt. Acta **28**, 1359 (1991).
5. I. V. Anisimov, S. M. Kozel, and G. R. Lokshin, Opt. Spectrosc. **27**, 258 (1969).
6. A. P. Vladimirov, *Dynamic Speckle-Interferometry of Deformable Bodies* (Ural Otd. RAN, Yekaterinburg, 2004).
7. E. Marom, *Golographic Nondestructive Investigations* (Mashinostroenie, Moscow, 1979), pp. 164–194.
8. E. Marom and R. K. Muller, Int. J. Nondestr. Test. **3**, 171 (1971).
9. V. P. Kozubenko, V. A. Potichenko, and Yu. S. Borodin, Probl. Prochn., No. 7, 103 (1989).
10. A. P. Vladimirov, I. S. Kamantsev, A. V. Ishchenko, V. E. Veselova, E. S. Gorkunov, S. V. Gladkovskii, and S. M. Zadvorkin, Deform. Razrushenie Mater., No. 1, 21 (2015).
11. D. Broek, *Elementary Engineering Fracture Mechanics* (Martinus Nijhoff, Dordrecht, 1986).
12. N. A. Klevtsova, O. A. Frolova, and G. V. Klevtsov, *Fracture of Austenitic Steels and Martensitic Transformations in Plastic Zones* (Izd. Akad. Estestvoznaniya, Moscow, 2005).

Translated by K. Shakhlevich